Colloidal Crystal Templating

DOI: 10.1002/anie.200705403

Bioinspired Fabrication of 3D Ordered Macroporous Single Crystals of Calcite from a Transient Amorphous Phase**

*Cheng Li and Limin Qi**

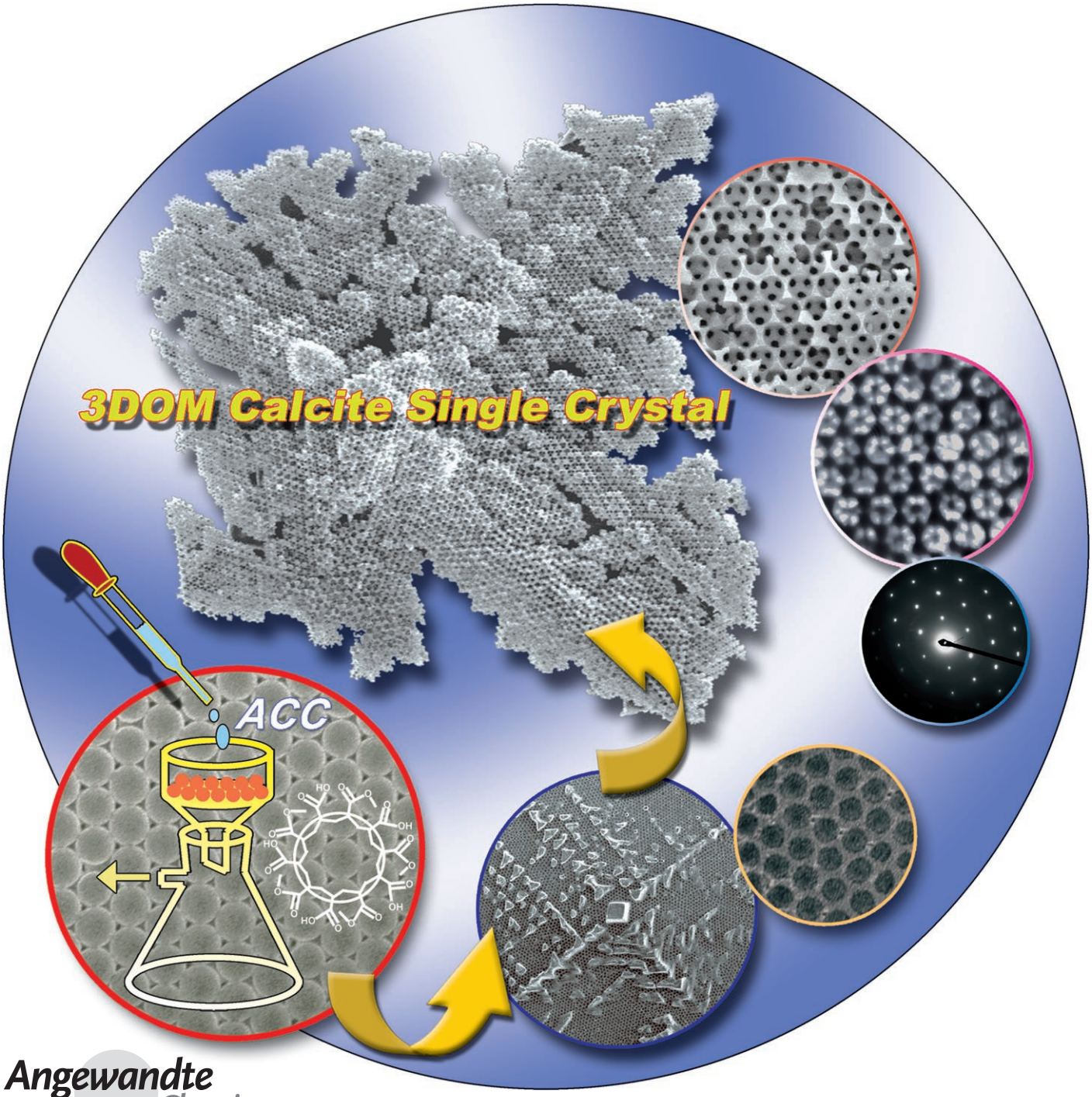

The development of bottom-up crystallization strategies to fabricate single crystals patterned on the micro- and nanometer scale is of great technological significance, as these patterned structures are important components in various electronic, sensory, and optical devices as well as in functional materials.[1,2] Particularly, the preparation of three-dimensionally (3D) ordered porous inorganic single crystals with well-defined structures and pore sizes remains an attractive challenge, because it is difficult to maintain such complex structural features on the micro- or nanometer scale without losing single-crystalline character. On the other hand, biological systems are good at producing large single-crystalline minerals with intricate architectures; moreover, most organisms form minerals exhibiting a precisely oriented crystallography as well as a sculpted shape.[3] In particular, as one of the most abundant biominerals, calcium carbonate ($CaCO_3$) often demonstrates complex single-crystalline structures, such as the three-dimensionally sculpted conformations of the calcite skeletal plates of echinoderms[4a] and coccoliths.[4b]

Biomineralization is generally considered to be an elaborate concerto orchestrated by both an insoluble organic matrix and soluble biomacromolecules.[5] In vitro approaches employing Langmuir monolayers,[6] self-assembled monolayers (SAM),[7] reverse microemulsions,[8] complex micelles,[9] and self-assembled bundles[10] as soft templates, as well as acidic biomolecules[11] or synthetic polymers[12] as growth modifiers have been explored extensively to exert control over crystallization of calcium carbonate. Recently, it has been revealed that organisms may use amorphous calcium carbonate (ACC) as a metastable precursor to form single crystals with complex shapes;[13] moreover, ACC has been found in many bioinspired crystallization experiments.[12d] One of the advantages of the amorphous-to-crystalline strategy is that the disordered and hydrated phase can be easily molded into any shape defined by spatial constraints. This strategy borrowed from nature has recently been exploited in vitro to fabricate crystalline $CaCO_3$ thin films[14] and cylindrical calcite single crystals.[15] Notably, large micropatterned calcite single crystals were fabricated through 2D-template-directed crystallization of a transient ACC phase,[1a] whereas large calcite single crystals with a complex pore structure were prepared by templating sea urchin spines;[2] nevertheless, the obtained porous calcite single crystals always exhibited micrometer-sized patterns. On the other hand, calcite single crystals with porous or patterned surfaces were obtained using colloidal spheres[16a] or colloidal monolayers[16b] as templates; however, there were essentially no pores inside the crystals. It is noted that surface-functionalized latex particles have recently been incorporated into ZnO single crystals.[17] Despite all the efforts devoted to sculpting the shape with hard templates, well-defined 3D conformations with precision at the submicrometer or nanometer scale have not, to date, been built within a calcite single crystal.

Colloidal crystals are generally 3D close-packed assemblies of monodisperse colloidal spheres, which have been widely used as sacrificial templates to fabricate 3D ordered macroporous (3DOM) materials.[18] Nevertheless, the existing procedures for the fabrication of 3DOM materials always lead to polycrystalline 3D networks; this result is largely related to a lack of control over crystallization during either the precursor infiltration or template removal processes.[19] Herein, we present a novel approach to generate for the first time 3DOM calcite single crystals, combining the amorphous-to-crystalline strategy with the use of colloidal crystals as 3D structured templates. We demonstrate that it is feasible for $CaCO_3$ to form single crystals with a well-defined 3DOM structure and controlled crystal orientation via a transient amorphous phase through specific surface functionalization of the colloidal crystal template and delicate control of the manner of introducing the ACC precursor.

The fabrication of 3DOM calcite single crystals was achieved by infiltration of the ACC precursor into polymer colloidal crystals with subsequent drying, dissolving in THF, and calcination at 450 °C (Scheme 1). Monodisperse poly-

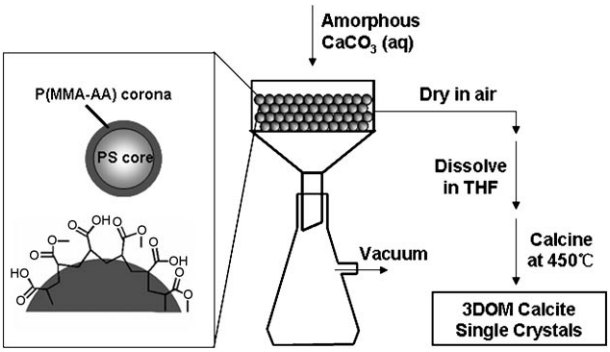

Scheme 1. Fabrication of 3DOM calcite single crystals by templating colloidal crystals of P(St-MMA-AA) spheres carrying a carboxylate corona.

(styrene–methyl methacrylate–acrylic acid) (P(St-MMA-AA)) colloidal spheres (ca. 450 nm in diameter), which have a polystyrene (PS) core and a carboxylate corona,[20] were assembled into 3D colloidal crystals on a filter membrane (see Figure S1 in the Supporting Information). Then, a freshly prepared ACC dispersion was added dropwise to the colloidal crystal film mounted on a Büchner funnel under vacuum, leading to the deposition and crystallization of ACC within the interstices of the colloidal crystals.

A mineral–polymer composite film was obtained after 12 drops (ca. 0.5 mL) of the ACC dispersion was infiltrated into the polymer colloidal crystals. As shown in Figure S2 in the Supporting Information, the X-ray diffraction (XRD) pattern of this film exhibits a sharp peak corresponding to the (104)

[*] C. Li, Prof. L. Qi
Beijing National Laboratory for Molecular Sciences (BNLMS)
State Key Laboratory for Structural Chemistry of Unstable and Stable Species
College of Chemistry, Peking University
Beijing 100871 (China)
Fax: (+86) 10-62751708
E-mail: liminqi@pku.edu.cn

[**] This work was supported by NSFC (20325312, 20673007, 20473003, and 50521201) and MOST (2007CB936201).

Supporting information for this article is available on the WWW under http://www.angewandte.org or from the author.

reflection of calcite along with a broad hump arising from the colloidal crystal template (see Figure S1 in the Supporting Information), thus indicating the formation of highly orientated calcite crystals with a large coherence length and with their {104} planes predominantly parallel to the surface of the colloidal crystal template. After the template was removed by sequential dissolution and calcination, the product was dispersed on a glass slide for the XRD characterization, which shows that only reflections ascribed to calcite can be observed, suggesting the formation of pure calcite crystals. The obtained crystals were characterized in detail by scanning electron microscopy (SEM, Figure 1). Figure 1a shows a top view of a piece of crystal, which exhibits a flat, dendritic morphology with two pronounced backbones that are perpendicular to each other and longer than 50 μm. A rhombohedral core lies at the intersection of the two crossed backbones, with the two diagonals of the top rhombus along the two backbones. An enlarged image (Figure 1b) reveals an interconnected network of spherical voids imprinted in the crystal, inheriting the *hcp* order of the colloidal crystal template. Some small ridges protrude on the flat surface, reflecting the dendritic characteristics of the whole crystal. Figure 1c presents a typical bottom view of the obtained flat dendritic crystals, which shows that the central part is considerably thicker than the peripheral regions. An enlarged image (Figure 1d) clearly shows that the crystal is entirely perforated. A high-magnification image (Figure 1e) exhibits the well-defined, 3D ordered macropores with a pore size of approximately 445 nm, slightly smaller than the original colloidal spheres. A side view of the crystal (Figure 1f) suggests that the relatively thinner peripheral region with the 3DOM structure has a thickness of about 2 μm. Namely, at least five layers of the colloidal spheres were replicated by the flat calcite crystal at the peripheral regions.

Amazingly, while the flat dendritic crystal is perforated by 3D ordered macropores, the complex calcite structure actually has a single-crystalline nature, which is revealed by the related transmission electron microscopy (TEM) and polarized-light optical microscopy characterizations (Figure 2). Figure 2a shows a low-magnification TEM image

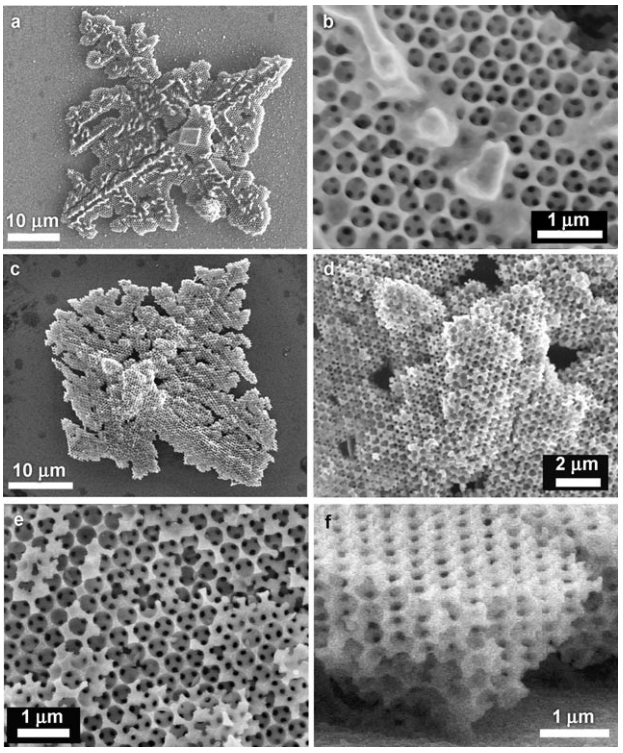

Figure 1. SEM images of 3DOM calcite single crystals formed from an ACC dispersion with a concentration of 8 mM: a,b) top view; c–e) bottom view; f) side view.

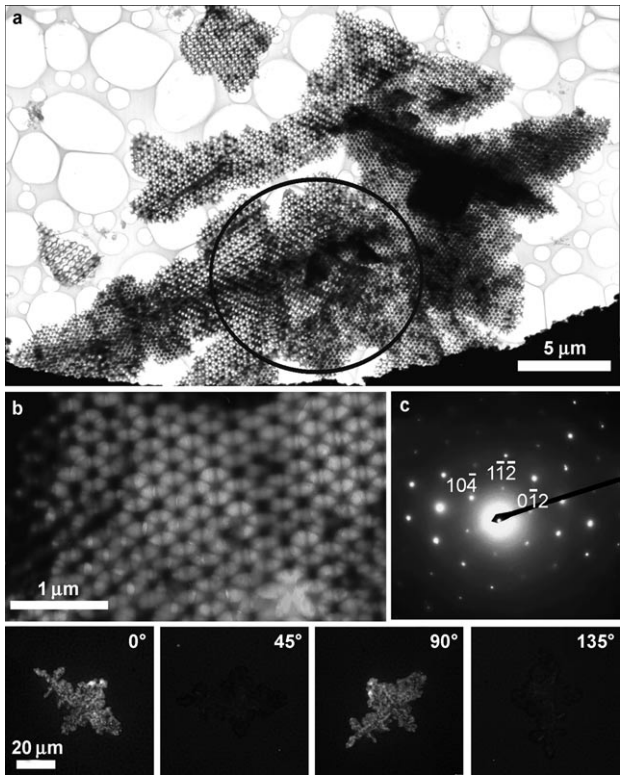

Figure 2. TEM images (a,b) and ED pattern (c) of 3DOM calcite single crystals formed from an ACC dispersion with a concentration of 8 mM: a) overview; b) an enlargement of (a); c) ED pattern corresponding to the circled area in (a). d) Polarized-light micrograph of a 3DOM calcite single crystal with different rotation angles.

of a typical 3DOM calcite crystal. The hexagonally aligned macropores inheriting the (111) planes of the colloidal crystal template can be clearly identified in the enlarged image (Figure 2b), thus indicating that the top surface of the inverse colloidal crystal is perpendicular to the electron beam. Figure 2c presents the electron diffraction (ED) pattern corresponding to a large selected area covering a major part of the dendritic crystal, which exhibits a set of sharp spots ascribed to the [421] zone axis of calcite. Indeed, the ED data obtained from other regions of the crystal showed exactly the same patterns. For a rhombohedral calcite crystal, the angle between the [421] direction and the normal direction of the (104) plane is calculated to be as small as 0.74°. (Note that for noncubic structure systems, the Miller index for the direction perpendicular to a crystal plane may not be the same as the

Miller index for the corresponding atomic plane.[21]) Hence, the crystal plane perpendicular to the electron beam is assigned to be the (104) plane, thus indicating that the 3DOM structure is actually a calcite single crystal with the (104) plane parallel to the top surface of the original colloidal crystal. Actually, almost all the 3DOM crystals exhibiting (111) oriented macropores show the ED pattern attributed to the [421] zone axis of calcite, confirming that the obtained 3DOM calcite single crystals are well-oriented. This result is consistent with the XRD data of the calcite–polymer composite film, which suggests the formation of (104) oriented calcite crystals, and also with the SEM top view of the 3DOM calcite crystals, which shows that the top (104) face of the rhombohedral core is just parallel to the top surface of the colloidal crystal template. The single-crystalline character of the 3DOM calcite crystals is further evidenced by the birefringence studies. Figure 2d presents four micrographs of an individual crystal rotated between two crossed polarizers at different angles, which shows that the entire structure switches between totally light and dark when rotated 45° from a certain start angle. The polarized-light micrographs with a continuous 360° rotation were recorded in a video clip (see the Supporting Information).

To elucidate the structural evolution process of the 3DOM calcite single crystals, different amounts of the ACC dispersion were infiltrated into the colloidal crystal template, and the resultant $CaCO_3$–polymer composite films were characterized by SEM (Figure 3). When one drop of the ACC dispersion was added, small patches (ca. 8 μm in size) that imprinted the $CaCO_3$ in the interstices of the colloidal crystals can be observed (Figure 3a). There is always a tuber or core particle at the center of each patch that protrudes from the relatively flat surface in surrounding areas (Figure 3b). When seven drops of the ACC dispersion were added, the $CaCO_3$ imprints developed the rudimentary appearance of a dendrite, with two crossed backbones, and the central core evolved into a faceted crystal with a diamondlike top face (Figure 3c). Finally, after 12 drops of the ACC dispersion were added, the central core evolved into a well-defined rhombohedron characteristic of a {104} oriented calcite crystal, and the $CaCO_3$ imprints developed into large dendrites exhibiting two pronounced backbones extending along the two crossed diagonals of the top rhombus of the central core (Figure 3d). After template removal, dendritic 3DOM calcite single crystals (Figure 1) would be obtained from these $CaCO_3$ imprints. The evident evolution of the central core from an irregular tuber to a well-defined rhombohedron may be considered as a signal of amorphous-to-crystalline transition, which is similar to the case of the early growth stage in sea urchin larval spicules.[1b] It may be noted that essentially all of the infiltrated ACC eventually crystallized into calcite crystals according to the polarized-light microscopy observations.

On the basis of the above observations, a possible formation process of the dendritic 3DOM calcite single crystals can be proposed (Scheme 2). Initially, the hydrated ACC granules carried by the water infiltrate quickly through the interstices of the colloidal crystals, where they fill the space evenly to the top to form a level imprint patch. At the center of the patch, a small tuber forms, which is followed by oriented nucleation and gradual evolution into a {104} oriented rhombohedral calcite core with its top (104) face parallel to the top surface of the colloidal crystal. The nucleation of the core crystal also triggers the amorphous-to-crystalline transition throughout the whole $CaCO_3$ imprint, resulting in a 3DOM calcite single crystal embedded in the template. Subsequent growth at the expense of ACC under non-equilibrium conditions leads to laterally dendritic expansion with a consistent crystallographic orientation. The formation of such symmetric, single-crystalline dendrites has been observed in many cases involving self-organized growth under non-equilibrium conditions.[22] It is worth noting that the oriented nucleation and crystallization process essentially resembles the formation of sea urchin larval spicules, where a *c*-axis-oriented rhombohedral calcite core evolves and induces the oriented crystallization of the whole triradiant spicule.[23] Finally, the 3DOM calcite single crystals result

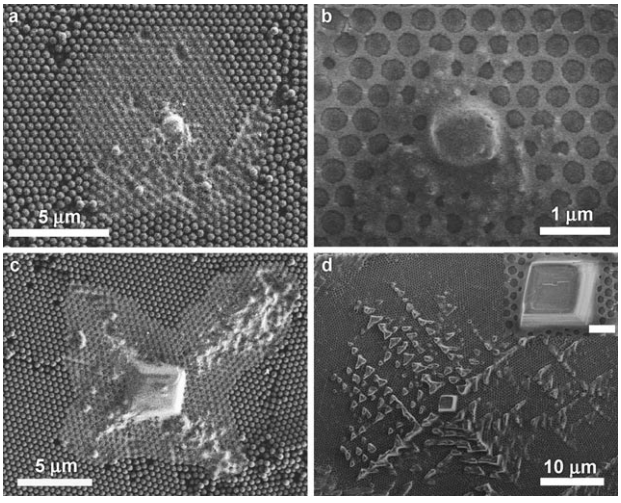

Figure 3. $CaCO_3$–polymer composite film formed after different volumes of the 8 mM ACC dispersion were dropped onto the template: a,b) 1 drop; c) 7 drops; d) 12 drops. Part (b) is an enlargement of the central region in (a). Inset in (d) is a enlargement of the rhombohedron in the center. The scale bar in the inset of (d) is 1 μm.

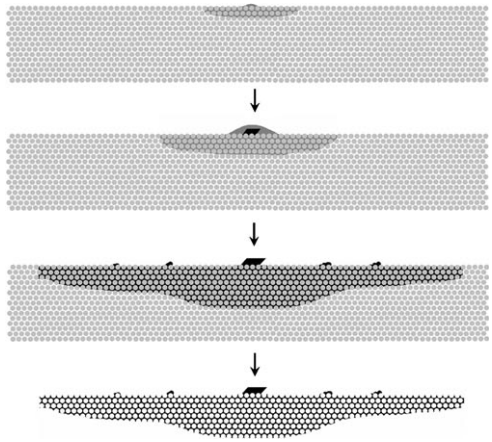

Scheme 2. Formation of flat 3DOM calcite single crystals.

from dissolving the latex particles in THF; further calcination at 450 °C would ensure complete removal of the organic material without changing the crystallinity of the calcite crystals.

Actually, the amorphous-to-crystalline pathway is crucial for the formation of 3DOM calcite single crystals, which is supported by the experimental data obtained from synthesis using the $CaCO_3$ precursor solution/dispersion at different concentrations. It has been reported that the mixed $CaCl_2$ and Na_2CO_3 solution with a $CaCO_3$ concentration below 3 mM is a transparent solution without spontaneous $CaCO_3$ precipitation.[15b] When a transparent solution containing 3 mM $CaCO_3$ was used for infiltration into the colloidal crystal template, most of the solution was directly sucked through the template, and only some rhombohedral calcite crystals nucleated on top of the template, resulting in concave hemispherical patterns imprinted on the surfaces that were in direct contact with the colloidal spheres (Figure 4a). When the $CaCO_3$ concentration in the mixed $CaCl_2/Na_2CO_3$ solution was increased to 4 mM, a translucent dispersion formed spontaneously, thus indicating the generation of transient ACC particles. If this ACC dispersion was introduced into the colloidal crystal template, the direct nucleation and growth of calcite crystals on the surface of the colloidal crystal template was prevented, (Figure 4b) and small $CaCO_3$ patches imprinted in the template were evident (Figure 4c). After template removal, rhombohedral 3DOM calcite single crystals were obtained (Figure 4d). An increase of the $CaCO_3$ concentration in the ACC dispersion to 8 mM resulted in the formation of larger dendritic 3DOM calcite single crystals embedded in the template, as shown in Figure 3d. However, a further increase of the $CaCO_3$ concentration above 25 mM would result in fast precipitation of calcite crystals in the solution. These results imply that ACC, a metastable phase, may well act as a temporary storage site that can efficiently feed calcium carbonate, not ions, into the template where they might undergo oriented nucleation and crystallization to form calcite single crystals within a limited space.

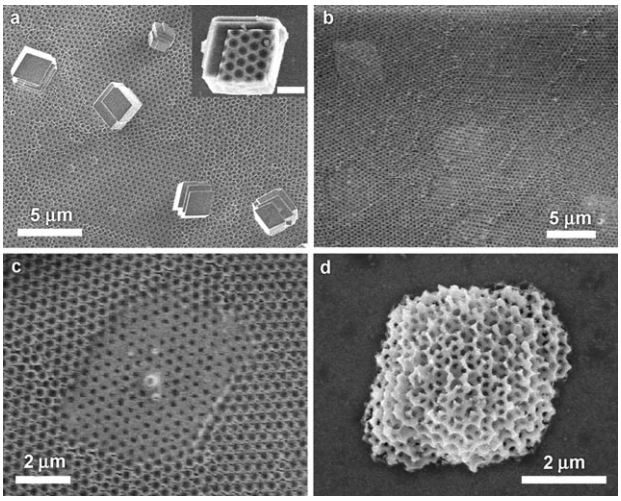

Figure 4. SEM images of calcite crystals formed by introducing a transparent solution containing 3 mM $CaCO_3$ (a) and a translucent ACC dispersion containing 4 mM $CaCO_3$ (b–d) into the colloidal crystal template. a–c) With the template; d) after removal of the template. The inset in (a) shows the opposite face of the rhombohedral crystal after removal of the template; the scale bar is 1 μm.

It was found that specific surface functionalization of the colloidal crystal template and delicate control of the manner of introduction of the ACC precursor are essential for the successful fabrication of 3DOM calcite single crystals. First, the carboxylate functional groups on the surfaces of the P(St-MMA-AA) colloidal crystal template favored the adsorption and deposition of ACC on the template surfaces and hence the filling of the template interstices with ACC, thus leading to the formation of calcite single crystals upon nucleation and crystallization. In contrast, only irregular calcite crystals grew on the top surface of the colloidal crystal template when a colloidal crystal assembled from polystyrene spheres (PS) without surface carboxylate groups was used as the template under otherwise similar synthesis conditions (see Figure S3 in the Supporting Information). Second, the introduction of the ACC precursor by vacuum-assisted filtration could favor a rapid feeding of the transient ACC phase to crystallization sites, thus avoiding the direct nucleation and growth of calcite crystals on the top surface of the template. This explanation is supported by the fact that only rhombohedral calcite crystals were deposited on the top surface of template when the P(St-MMA-AA) colloidal crystal template was just placed in the ACC dispersion for the crystallization (see Figure S4 in the Supporting Information).

In conclusion, we have demonstrated a direct, bottom-up fabrication of unique 3DOM calcite single crystals with controlled orientation and well-defined nanopatterns by exploiting the amorphous-to-crystalline strategy in combination with the colloidal crystal templating method. It was shown that the calcite single crystals that formed in the colloidal crystal template evolved from small patches to large symmetric dendrites up to several tens of micrometers in size as the amount of ACC was increased. The success of our approach relies upon two key points, that is, the surface-functionalized template, which provided the affinity to ACC, and the vacuum-assisted filtration process, which induced the filling of ACC in the interstices of the template. Since colloidal crystals represent a topologically complex confinement with resolution at the nanometer scale, our results suggest a general strategy for the design and fabrication of functional single-crystalline materials with desired nanopatterns, orientations, and shapes. Furthermore, the in vitro fabrication of such complex calcite single crystals could shed light on fundamental mechanisms that regulate nanoscale phenomena in biomineralization.

Received: November 25, 2007
Published online: February 25, 2008

Keywords: biomineralization · calcite · colloidal crystals · crystal growth · nanostructures

[1] a) J. Aizenberg, D. A. Muller, J. L. Grazul, D. R. Hamann, *Science* **2003**, *299*, 1205; b) J. Aizenberg, *Adv. Mater.* **2004**, *16*, 1295.

[2] a) R. J. Park, F. C. Meldrum, *Adv. Mater.* **2002**, *14*, 1167; b) W. Yue, A. N. Kulak, F. C. Meldrum, *J. Mater. Chem.* **2006**, *16*, 408; c) B. Wucher, W. Yue, A. N. Kulak, F. C. Meldrum, *Chem. Mater.* **2007**, *19*, 1111.
[3] a) S. Weiner, I. Sagi, L. Addadi, *Science* **2005**, *309*, 1027; b) K. M. Towe, *Science* **2006**, *311*, 1554.
[4] a) J. Aizenberg, A. Tkachenko, S. Weiner, L. Addadi, *Nature* **2001**, *412*, 819; b) J. R. Young, S. A. Davis, P. R. Bown, S. Mann, *J. Struct. Biol.* **1999**, *126*, 195.
[5] S. Mann, *Biomineralization: Principles and Concepts in Bioinorganic Materials Chemistry*, Oxford University Press, Oxford, **2001**.
[6] a) S. Mann, B. R. Heywood, S. Rajam, J. D. Birchall, *Nature* **1988**, *334*, 692; b) B. R. Heywood, S. Mann, *Adv. Mater.* **1994**, *6*, 9; c) S. Cavalli, D. C. Popescu, E. E. Tellers, M. R. J. Vos, B. P. Pichon, M. Overhand, H. Rapaport, N. A. J. M. Sommerdijk, A. Kros, *Angew. Chem.* **2006**, *118*, 753; *Angew. Chem. Int. Ed.* **2006**, *45*, 739; d) M. Fricke, D. Volkmer, *Top. Curr. Chem.* **2007**, *270*, 1.
[7] a) J. Aizenberg, A. J. Black, G. M. Whitesides, *Nature* **1999**, *398*, 495; b) Y.-J. Han, L. M. Wysocki, M. S. Thanawala, T. Siegrist, J. Aizenberg, *Angew. Chem.* **2005**, *117*, 2438; *Angew. Chem. Int. Ed.* **2005**, *44*, 2386; c) H. Li, L. A. Estroff, *J. Am. Chem. Soc.* **2007**, *129*, 5480; d) J. R. I. Lee, T. Y.-J. Han, T. M. Willey, D. Wang, R. W. Meulenberg, J. Nilsson, P. M. Dove, L. J. Terminello, T. van Buuren, J. J. De Yoreo, *J. Am. Chem. Soc.* **2007**, *129*, 10370.
[8] a) M. Li, S. Mann, *Adv. Funct. Mater.* **2002**, *12*, 773; b) S. Thachepan, M. Li, S. A. Davis, S. Mann, *Chem. Mater.* **2006**, *18*, 3557.
[9] L. Qi, J. Li, J. Ma, *Adv. Mater.* **2002**, *14*, 300.
[10] S. Burazerovic, J. Gradinaru, J. Pierron, T. R. Ward, *Angew. Chem.* **2007**, *119*, 5606; *Angew. Chem. Int. Ed.* **2007**, *46*, 5510.
[11] a) P. K. Ajikumar, S. Vivekanandan, R. Lakshminarayanan, S. D. S. Jois, R. M. Kini, S. Valiyaveettil, *Angew. Chem.* **2005**, *117*, 5612; *Angew. Chem. Int. Ed.* **2005**, *44*, 5476; b) A. Sugawara, T. Nishimura, Y. Yamamoto, H. Inoue, H. Nagasawa, T. Kato, *Angew. Chem.* **2006**, *118*, 2942; *Angew. Chem. Int. Ed.* **2006**, *45*, 2876; c) S. E. Wolf, N. Loges, B. Mathiasch, M. Panthofer, I. Mey, A. Janshoff, W. Tremel, *Angew. Chem.* **2007**, *119*, 5716; *Angew. Chem. Int. Ed.* **2007**, *46*, 5618.
[12] a) H. Cölfen, L. Qi, *Chem. Eur. J.* **2001**, *7*, 106; b) X.-H. Guo, S.-H. Yu, G.-B. Cai, *Angew. Chem.* **2006**, *118*, 4081; *Angew. Chem. Int. Ed.* **2006**, *45*, 3977; c) A. N. Kulak, P. Iddon, Y. Li, S. P. Armes, H. Cölfen, O. Paris, R. M. Wilson, F. C. Meldrum, *J. Am. Chem. Soc.* **2007**, *129*, 3729; d) H. Cölfen, *Top. Curr. Chem.* **2007**, *271*, 1.
[13] a) L. Addadi, S. Raz, S. Weiner, *Adv. Mater.* **2003**, *15*, 959; b) Y. Politi, T. Arad, E. Klein, S. Weiner, L. Addadi, *Science* **2004**, *306*, 1161; c) L. Addadi, D. Joester, F. Nudelman, S. Weiner, *Chem. Eur. J.* **2006**, *12*, 980; d) Y. Ma, S. Weiner, L. Addadi, *Adv. Funct. Mater.* **2007**, *17*, 2693.
[14] a) D. Volkmer, M. Harms, L. Gower, A. Ziegler, *Angew. Chem.* **2005**, *117*, 645; *Angew. Chem. Int. Ed.* **2005**, *44*, 639; b) D. C. Popescu, E. N. M. van Leeuwen, N. A. A. Rossi, S. J. Holder, J. A. Jansen, N. A. J. M. Sommerdijk, *Angew. Chem.* **2006**, *118*, 1794; *Angew. Chem. Int. Ed.* **2006**, *45*, 1762; c) S. Tugulu, M. Harms, M. Fricke, D. Volkmer, H.-A. Klok, *Angew. Chem.* **2006**, *118*, 7619; *Angew. Chem. Int. Ed.* **2006**, *45*, 7458.
[15] a) E. Loste, F. C. Meldrum, *Chem. Commun.* **2001**, 901; b) E. Loste, R. J. Park, J. Warren, F. C. Meldrum, *Adv. Funct. Mater.* **2004**, *14*, 1211.
[16] a) C. Lu, L. Qi, H. Cong, X. Wang, J. Yang, L. Yang, D. Zhang, J. Ma, W. Cao, *Chem. Mater.* **2005**, *17*, 5218; b) N. B. J. Hetherington, A. N. Kulak, K. Sheard, F. C. Meldrum, *Langmuir* **2006**, *22*, 1955.
[17] R. Muñoz-Espi, Y. Qi, I. Lieberwirth, C. M. Gomez, G. Wegner, *Chem. Eur. J.* **2006**, *12*, 118.
[18] a) O. D. Velev, A. M. Lenhoff, *Curr. Opin. Colloid Interface Sci.* **2000**, *5*, 56; b) A. Stein, R. C. Schroden, *Curr. Opin. Solid State Mater. Sci.* **2001**, *5*, 553; c) M. L. K. Hoa, M. Lu, Y. Zhang, *Adv. Colloid Interface Sci.* **2006**, *121*, 9, and references therein.
[19] H. Yan, C. F. Blanford, B. T. Holland, W. H. Smyrl, A. Stein, *Chem. Mater.* **2000**, *12*, 1134.
[20] H. Cong, W. Cao, *Langmuir* **2003**, *19*, 8177.
[21] Y. Ding, Z. L. Wang, *J. Phys. Chem. B* **2004**, *108*, 12280.
[22] H. Imai, *Top. Curr. Chem.* **2007**, *270*, 43.
[23] E. Beniash, L. Addadi, S. Weiner, *J. Struct. Biol.* **1999**, *125*, 50.

